Research article

A comparative study of radiation models on propane jet fires based on experimental and computational studies

Hossein Mashhadimoslem [a], Ahad Ghaemi [a],[*], Adriana Palacios [b],[**]

[a] School of Chemical, Petroleum and Gas Engineering, Iran University of Science and Technology, Narmak, 16846, Tehran, Iran
[b] Department of Chemical, Food and Environmental Engineering, Fundacion Universidad de las Americas, Puebla, 72810, Mexico

A B S T R A C T

Radiation as a consequence of jet fires is one of the significant parameters in process industry events. In the present work, the open field vertical propane jet fire was studied via experimental and computational fluid dynamics (CFD). The predicted values of radiation were verified at three locations in the horizontal direction from the jet fire. In the simulation section, four radiation models of Monte Carlo (MC), P-1, Discrete Transfer (DT), and Rosseland were applied to find the fine model for simulating the jet fire. Shear Stress Transport (SST) and Eddy Dissipation Concept (EDC) models are employed for combustion and turbulence, respectively. The estimated data by the simulation demonstrated that the MC radiation is better than the other models with an average error of 5% for predicted incident radiation from the jet flame axis. Also, the P-1 radiation model had an above 65% error at around the jet fire, but due to the error of less than 15% estimated by MC and DT models, these radiation models could simulate the jet flame radiation. The simulation outcomes proved that the Rosseland radiation model is not applicable owing to a lack of accurate temperature prediction.

1. Introduction

Jet fire thermal hazards, due to the radiation effect, can be very catastrophic. Jet fires that could occur in congested arrangements of process units have a risk of a domino effect owing to the flame collision with other equipment, which could result in irreparable property damages. Examining and estimating the influences of radiation models assisted by the simulation for a jet fire can prevent future accidents in industrial processes. Prediction of conduct and radiation of the jet fire phenomena are extremely important in the gas and oil industries. For example, during the location of equipment to avoid the domino effect in industrial events, precise prediction of jet fires radiation is important (Cumber and Fairweather, 2005). Radiation is a heat transfer that is bounded by a relatively narrow "window" electromagnetic spectrum through space with electromagnetic waves. The convection mechanism is governing at low temperatures (<150–200 °C). When the temperature is more than 400 °C, the radiation heat transfer mechanism is governing (Hottel and Hawthorne, 1948; Brzustowski, 1973; Yeoh and Yuen, 2009).

Numerous empirical and computational researches have been developed on jet flame radiation (Brzustowski, 1973; McMurray, 1982; Galant et al., 1984; Schuller et al., 1983; Hustad and Sonju, 1986; McCaffrey et al., 1986a; Chamberlain, 1987; McCaffrey et al., 1988b; Cook et al., 1990; Lowesmith et al., 2007; Palacios et al., 2009, 2012; Palacios Rosas, 2011; Palacios and Casal, 2011; Gomez-Mares et al., 2009, 2010) based their studies on the solid flame model, using natural gas or propane as a fuel. A line source model has been proposed by Zhou and Jiang, (2016) to anticipate the radiation of horizontal propane jet fires, where different shapes such as a cylinder, a frustum of a cone, an ellipse, and a kite were suggested for the jet flame shape. As part of the development of radiation simulation models, studies of different radiation simulation models are shown in Table 1.

Most of the researches has been conducted on the empirical and CFD simulation study of jet fire radiation works with different approaches. In the stated studies, there is a lack of simulation data on the effect of radiation models in the vicinity of propane jet fires. Hence, the aim of the current study is to validate CFD simulations of jet fires, using four different radiation models (i.e., the Monte Carlo (MC), Rosseland, P-1, and discrete transfer (DT)) and experimental jet flame data, for select the better than radiation model. It is possible to accurately estimate the damage caused by thermal flux to equipment by accurately calculating and predicting jet fire radiation.

---

* Corresponding author.
** Corresponding author.
  E-mail addresses: aghaemi@iust.ac.ir (A. Ghaemi), adriana.palacios@udlap.mx (A. Palacios).

Table 1. Summary of several experimental and CFD simulation works on jet fires with different simulation approaches.

Reference	Simulation approach	Fuel Type	Jet Orientation	Remark
Li and Modest (2003)	Finite volume code. (FV)	Methane	Horizontal	Simulation based on the probability density function (PDF) method.
Liu et al. (2004)	CFD with ANSYS-CFX code.	Iso-propanol	Vertical	Investigation of the impact of air conditioning in a jet fire in a closed area.
Cumber and Fairweather (2005)	CFD framework with GENMIX program	Methane	Vertical	Simulated the jet flame based on flame emissions such as gray gas, mixed gray gas, total transmittance, non-homogeneous (TTNH), exponential wideband, and statistical narrow band models.
Cumber and Spearpoint (2006)	CFD framework.	Propane	Vertical	Evaluated the influence of jet fire for determining a flame length and comparing the data resulted from the thermal camera utilized throughout the experiments.
Habibi et al. (2007)	CFD framework.	Methane/Hydrogen	Vertical	Simulated the furnace fire based on Realizable k-ε turbulence, Finite Rate/ Eddy-Dissipation combustion model and compared the radiation models such as Rosseland, P-1, and Discrete Ordinates (DO).
Rusch et al. (2008)	CFD with CFX code.	Propane	Vertical and Horizontal	Examined the impact of turbulence models on fire simulation with the hot jet in crossflow in the long tunnel.
Mehta et al. (2010)	CFD framework.	methane (94%), and methane–ethylene mixture (90–10%)	Vertical	Investigated turbulent jet flame radiation based on the RTE solver combination with transported PDF method coupled with soot model and MC radiative equations.
Wang and Guo (2011)	CFD with Fire Dynamics Simulator (FDS) code.	Heptane	Vertical	Examined the jet fire with the LES turbulence model due to the leakage of fluids.
Lowesmith and Hankinson (2012)	Thermal imaging	Natural gas/hydrogen mixture	Horizontal	Investigated temperature profile and incident radiation from jet flame experimentally.
Wang (2012)	CFD with FDS code.	Heptane	Vertical	Investigated the large eddy simulation (LES) turbulence model with the combustion models.
Yuen et al. (2013)	CFD code.	Propane	Vertical	Studied a jet fire in a large room using the SGS turbulence model.
Cumber and Onokpe (2013)	finite volume mesh with CFD code.	Hydrogen	Vertical	Simulated of the jet fire spectral emission based on RADCAL radiation model.
Zárate et al. (2014)	Thermal imaging and CFD code.	Propane	Vertical	The concept of solid flame was utilized to decrease the amount of computation.
Wang et al. (2014)	CFD with Fire FOAM code.	Hydrogen and hydrogen/methane mixture	Vertical and Horizontal	Studied the thermal radiation flux, flame length, and the influence of the radiation reflected from the ground.
Jang et al. (2015)	CFD with Kameleon Fire Ex (KFX) code.	Hydrogen	Horizontal	Surveyed the influence of jet fire radiation in the pipeline on the structure.
Taghinia et al. (2016)	CFD with house code.	Propane	Horizontal	Examined the heat transfer with the RANS k-ε model due to the contact of a jet fire from the wall.
Petera and Dostál (2016)	CFD with ANSYS Fluent code.	Propane	Vertical	

Table 1 (*continued*)

Reference	Simulation approach	Fuel Type	Jet Orientation	Remark
				Evaluated the LES turbulence suggested better predictions than the RANS turbulence models.
Jang and Jung (2016)	CFD with KFX code.	Hydrogen	Vertical	Investigated the jet fire resulted from hydrogen leakage from a pipe in the process plant.
Mbainguebem et al. (2017)	CFD with Open FOAM code.	Methane	Vertical	Investigated the soot formation in a jet fire.
Consalvi and Nmira (2017)	Optically Thin Fluctuation Approximation (OTFA) with CFD code.	Ethylene	Vertical	Investigated absorption Turbulence-Radiation Interactions (TRI) on radiative heat transfer.
Baalisampang et al. (2017)	CFD with FDS.	Floating Liquefied Natural Gas	Vertical and Horizontal	Examined the jet fires' incidence in the Floating LNG (FLNG) facility.
Jang and Choi (2017)	CFD with KFX code.	Propane	Vertical	Evaluated the influence of the jet fire due to gas discharge.
Hussein et al. (2018)	CFD code.	Hydrogen	Vertical	Simulated the real and lab scale jet flames via EDC combustion, DO radiation, and RNG k-ε, Realizable k-ε, SST models.
Xiao et al. (2018)	CFD GASFLOW-MPI code with FLUENT	Hydrogen	Vertical	CFD GASFLOW-MPI code for radiation with the k-ε turbulence and Eddy Dissipation Model (EDM) combustion models was used.
Liu et al. (2019)	Thermal imaging	Propane	Horizontal	Correlated heat release rate based on jet flame Froude number experimentally.
Cirrone et al. (2019a)	CFD code.	Hydrogen	Vertical	Simulated the flame according to EDC combustion, and DO radiation, Realizable k-ε turbulence models.
Cirrone et al. (2019b)	CFD code.	Hydrogen	Horizontal	Simulated the flame length according to DO radiation, Realizable k-ε turbulence, EDC combustion models.
Mashhadimoslem et al. (2020a)	CFD code coupled with CFX.	Propane	Vertical	Simulated the jet flame shape according to k-ε, SST, BSL, and Realizable k-ε turbulences, EDC combustion, and Monte Carlo radiation models.
Mashhadimoslem et al. (2020b)	CFD code coupled with CFX.	Hydrogen and Propane	Vertical	Simulated the jet flame radiation according to SST turbulences, EDC combustion, and Monte Carlo radiation models.
Palacios and Rengel (2020)	CFD with FDS code.	Propane	Vertical and Horizontal	Examined the radiation influence of the jet fire due to surface emissive powers.
Wang et al. (2021)	Thermal imaging	Propane	Horizontal	Investigated temperature profile of jet flame on vertical plate

2. Radiation model

Various solution methods have been advanced over the years to predict the incident heat radiation. These procedures consist of several scientific and numerical techniques for estimation (Hottel and Hawthorne, 1948). Physical understanding of geometry is particularly important in selecting the governing equations involved in the heat transfer radiation to understand complex barriers in the radiative heat transfer analysis. Radiation modeling aims to solve the spectral Radiation Transfers Equation (RTE) for using the energy balance and the heat flux boundary condition at walls, containing the desired quantities as a source term of S_{rad} for radiation intensity. The spectral (RTE) can be as follows:

$$\frac{dI_\nu(r,s)}{ds} = -(K_{a\nu} + K_{s\nu})I_\nu(r,s) + K_{a\nu}I_b(\nu,T) + \frac{K_{s\nu}}{4\pi}\int_{4\pi} dI_\nu(r,s')\Phi(s \bullet s')d\Omega'$$
$$+ S_{rad} \tag{2}$$

where ν is the frequency, r is the position vector, s is the direction vector, s' is the path length, K_a is the coefficient of absorption, $K_{s\nu}$ is the scattering coefficient, I_b is the blackbody emission intensity, I_ν is the spectral radiative intensity, depending on the direction s and position r. T is the local absolute temperature, Ω is a solid angle, φ is an in-scattering phase function, and S_{rad} is the radiation intensity source term.

3. Numerical detail

3.1. Governing equations

The governing equations employed in the current study to simulate the jet flame are four Navier-Stokes equations for turbulent flow concerning the reaction (ANSYS CFX-Solver Theory Guide, 2017; Bird et al., 2007). These are as follows:
Conservation of mass:

$$\frac{\partial \rho}{\partial t} + \frac{\partial \rho u_i}{\partial x_i} = 0 \tag{3}$$

Conservation of momentum:

$$\frac{\partial \rho u_j}{\partial t} + \frac{\partial \rho u_i u_j}{\partial x_i} = -\frac{\partial p}{\partial x_j} + \frac{\partial \tau_{ij}}{\partial x_i} + f_i \tag{4}$$

Mass transfer balance:

$$\frac{\partial \rho \phi}{\partial t} + \frac{\partial \rho \phi u_i}{\partial x_i} = \frac{\partial}{\partial x_i}\left(\frac{\partial \phi}{\partial x_i}\right) + S_\phi \tag{5}$$

Conservation of energy:

$$\frac{\partial \rho h}{\partial t} + \frac{\partial \rho u_i h}{\partial x_i} = \frac{\partial}{\partial x_i}\left(\frac{1}{c_p} + \frac{\mu_t}{Pr_t}\frac{\partial h}{\partial x_i}\right) + S_{rad} \tag{6}$$

3.2. Turbulence model

The governing equations for the turbulence flow are according to the transport equations of the shear stress transport (SST) model. The SST model used to simulate jet fires is depicted in detail in Table 2. The Favre-Averaged Navier-Stokes equations coupled with the k-ω model are solved in the axial cylindrical coordinates, in which their constants are reported in Table 2 (Pope, 2001; ANSYS CFX-Solver Theory Guide; 2017).

3.3. Combustion model

Eddy Dissipation Concept model is employed as the combustion model (Jeon et al., 2015; Magnussen, 1981). A one-step reaction is considered for combustion. The soot formation is described by the Soot

Magnusson model connected to the vortex loss model. Jeon et al. (2015) and Magnussen (1981) resent the detail of the chemical reaction mechanism. The rate of reaction rate for the species i, i.e., R_i, is computed as follows:

$$R_i = \frac{\rho(\dot{\xi})^2}{\dot{\tau}[1 - (\dot{\xi})^3]}\left(\dot{Y}_i - Y_i\right) \tag{7}$$

$$\dot{\xi} = C_\xi \left(\frac{\nu\xi}{k^2}\right)^{1/4} \tag{8}$$

$$\dot{\tau} = C_\tau \left(\frac{\nu}{\xi}\right)^{1/2} \tag{9}$$

where Yi is the mass fraction of species through reaction after the time scale $\dot{\tau}$, $\dot{\xi}$ is the fine-scale length, and ν is the kinematic viscosity. C_τ and C_ξ are the constants of times scale and volume fraction with the values of 0.4082 and 2.1377, respectively.

3.4. Monte Carlo radiation model

The Monte Carlo (MC) model is a mathematical methodology for predicting radiative heat transfer with high precision. Due to the association of radiation with the involved media, this approach can be applied to some intricate 3D structures in Cartesian coordinates, some incident radiation on the optics, and complex physical phenomena. The MC model assumes that the differential angle of photon flux is proportional to radiation intensity and that the radiation field is a photon gas. The probability of a photon being absorbed in a given frequency is the Ka parameter for this gas. Accordingly, the average radiation intensity (I) is proportional to the distance of the photon per unit volume in unit time. As well as, q_ν is proportional to the radiant incidence of photons in the radial surface of r because the volumetric absorption is dependent on the photon absorption rate. The average radiation intensity can be estimated by multiplying the distance traveled in each element by following the

Table 2. Turbulence model equations (Pope, 2001; ANSYS CFX-Solver Theory Guide; 2017).

Transport Equations Shear Stress Transport (SST) Model
Kinematic Eddy Viscosity:
$\nu_T = \dfrac{a_1 k}{\max(a_1 \omega, SF_2)}$
Turbulence Kinetic Energy:
$\dfrac{\partial k}{\partial t} + U_j \dfrac{\partial k}{\partial x_i} = P_k - \dot{\beta}k\omega \dfrac{\partial}{\partial x_j}\left[(\nu + \sigma_k \nu_T)\dfrac{\partial k}{\partial x_j}\right]$
Specific Dissipation Rate:
$\dfrac{\partial \omega}{\partial t} + U_j \dfrac{\partial \omega}{\partial x_i} = aS^2 - \dot{\beta}\omega^2 + \dfrac{\partial}{\partial x_j}\left[(\nu + \sigma_k \nu_T)\dfrac{\partial \omega}{\partial x_j}\right] + 2(1-F_1)\sigma_{\omega 2}\dfrac{1}{\omega}\dfrac{\partial k}{\partial x_i}\dfrac{\partial \omega}{\partial x_i}$
Closure Coefficients and Auxiliary Relations:
$F_2 = \tanh\left(\left[\max\left(\dfrac{2\sqrt{k}}{\beta\omega y}, \dfrac{500\nu}{y^2\omega}\right)\right]^2\right)$
$P_k = \min\left[\tau_{ij}\dfrac{\partial U_i}{\partial x_j}, 10\dot{\beta}k\omega\right]$
$F_1 = \tanh\left(\left[\min\left(\max\left(\dfrac{2\sqrt{k}}{\beta\omega y}, \dfrac{500\nu}{y^2\omega}\right), \dfrac{4\sigma_{\omega 2}k}{CD_{k\omega}y^2}\right)\right]^2\right)$
$CD_{k\omega} = \max\left(2\rho\sigma_{\omega 2}\dfrac{1}{\omega}\dfrac{\partial k}{\partial x_i}\dfrac{\partial \omega}{\partial x_j}, 10^{-10}\right)$
$a = a_1 F + a_2(1-F)$
Model constants:
$\beta = 0.09, \alpha_1 = \dfrac{5}{9}, \beta_1 = \dfrac{3}{40}, \sigma_{k1} = 0.85, \alpha_2 = 0.44, \beta_2 = 0.0828, \sigma_{k2} = 1, \sigma_{\omega 2} = 0.856$

Note: F_1 and F_2 are blending functions that switches over to one within the boundary layer (k-ω model).

typical selection of photons. The usual choice of photons and their computation in each element will calculate the coefficient of time absorption by acquiring the overall absorption rate by conformity. By selecting a sample of photons and computing each element with the scattering coefficient's time period, the average intensity of the scattering could be calculated. Moreover, counting the number of photons occurring on a surface can determine the absorbed flux and average radiation flux.

3.5. P-1 radiation model

The spherical harmonics P-1 differential estimation is one of the calculation methods for the radiation transfer estimations. Nevertheless, this is a delicate approach to solve transfer problems for the calculation of radiation energy. Jeans (1917) firstly proposed the P-1 method to solve special problems in astrophysics studies. Differential estimation or P-1 is a reduction of the RTE model, which considers that the intensity of the isotropic radiation or direction is independent in a specific location of space. McCaffrey and Evans, (1988) presented the complete form of the radiation energy equation and the radiation model P-1. The spectral heat flux radiation in the diffusion term for an emitting, absorbing, and linearly dispersion medium, can be calculated as (ANSYS CFX-Solver Theory Guide; 2017):

$$q_{rv} = -\frac{1}{3(K_{av} - K_{sv}) - AK_{sv}}\nabla G_v \tag{10}$$

$$-\nabla \cdot \left(\frac{1}{3(K_{av} - K_{sv}) - AK_{sv}}\nabla G_v\right) = K_{av}(E_{av} - G_v) \tag{11}$$

where A is the linear anisotropy coefficient.

3.6. Discrete transfer radiative model

The discrete transfer radiative method (DT) was suggested by Gosman et al. (1982). The discrete transfer model considers that the radiation intensity is emitted through a solid angle by approximating the radius of radiation (ANSYS CFX-Solver Theory Guide; 2017). The DT method solves the radiative transfer equation of the RTE model for each ray from solid boundaries to another boundary in geometry. RTE equations describe radiation intensity fields in adsorption, diffusion, and dispersion field.

The DT method can calculate the intensity distribution in complex geometries as desired in three dimensions' media. The utilization of the discrete transfer model in ANSYS-CFX was according to the isotropic dispersion.

3.7. Rosseland radiation model

The Rosseland model is simplified by the RTE in the case of optically thick media that was originally derived by Rosseland (1936). The total heat flux of radiation in an optically thick and dispersion medium can be derived as follow (ANSYS CFX-Solver Theory Guide; 2017):

$$q_r = -\int_0^\infty \frac{4}{3\beta - CK_s}\nabla E_{bv}d_v \tag{12}$$

where β is the coefficient of extinction (e.g., absorption plus dispersion). The energy spectrum for the radiation emitted by a blackbody is E_{bv} and C is the speed of light in a vacuum. When the Rosseland estimation is defined into the energy transport equation, the heat flux radiation conduction could be integrated as follows (ANSYS CFX-Solver Theory Guide; 2017):

$$q = q_c + q_r \tag{13}$$

$$q = -(k + k_r)\nabla T \tag{14}$$

$$k_r = -\frac{16\sigma n^2 T^3}{3\beta} \tag{15}$$

where k and k_r are the thermal conductivity and the total radiative conductivity, respectively.

3.8. Radiative soot model

In the Eddy Dissipation Concept (EDC) model, soot is permitted to be created both in fine structures and the surroundings while soot oxidation is achieving location considerably in these structures. The soot and nucleus act as the homogeneous reactors given below (Kleiveland, 2005; Magnussen, 1989).

$$\frac{dY_{n/s}^*}{dt} = \dot{m}^*\left(Y_{n/s}^\circ - Y_{n/s}^*\right) + \omega_{n/s}^* \tag{16}$$

$$\omega_{n/s}^* = \omega_{n/s,f}^* + \omega_{n/s,c}^* \tag{17}$$

The mean reaction rates for soot and nucleus can be attained by the mass averaging the rates of reaction in the surroundings and fine structures.

$$\tilde{\omega}_{n/s} = \gamma^* x \omega_{n/s,f}^* + (1 - \gamma^* x)\omega_{n/s,f}^\circ + \gamma^* x \omega_{n/s,c}^* \tag{18}$$

The formation terms $\omega_{n/s,f}^*$ are given by Eqs. (19) and (20) (Kleiveland, 2005; Magnussen, 1989):

$$\omega_{nf,I} = \frac{1}{\rho}\frac{dn}{dt} = \frac{n_s}{\rho} + (f - g)Y_n - \rho\frac{g_s}{m_p}Y_n Y_s \tag{19}$$

$$\omega_{sf,I} = \frac{m_p}{\rho}\frac{ds}{dt} = (m_p a - b\rho Y_s)Y_n \tag{20}$$

The combustion terms are presented by Eq. (21) (Kleiveland, 2005; Magnussen, 1989):

$$\omega_{n/s,c}^* = \omega_{fu}^*\frac{\tilde{Y}_{n/s}}{\tilde{Y}_{fu}} \tag{21}$$

4. Experimental setup

In the present study, vertical propane fires in the open field have been simulated by Palacios et al. (2012) by four radiation models. The fuel was vertically released within a nozzle with an outlet size diameter of 12.75 mm. Three Schmidt–Boelterheatflow radiometers sensors measured the incident heat radiation from the jet flames, which were placed at three horizontal distances from the jet flame axis (i.e., 1.1 m, 3 m, and 5 m) and also at 1 m upon the release orifice nozzle. The maximum allowable operating body temperature of radiometers was 250 °C with a measurement range of 0–227 kW/m² and ±0.5% repeatability. When measuring thermal radiation intensity, the estimated experimental uncertainty is 3% at a 95% confidence level. For ranges up to 250 BTU ft^{-2}s^{-1}, the calibration expanded uncertainty for an approximate 95 % confidence trust level was 3%.

The uncertainty due to the experimental setup was estimated values were confirmed by the empirical data of Palacios et al. (2012). The scheme of the experimental setup is depicted in Figure 1.

4.1. Computational domain and solution algorithm

In the current work, the computational domain considers as the symmetrical axial cylinder containing a fuel inlet with a vertical circular
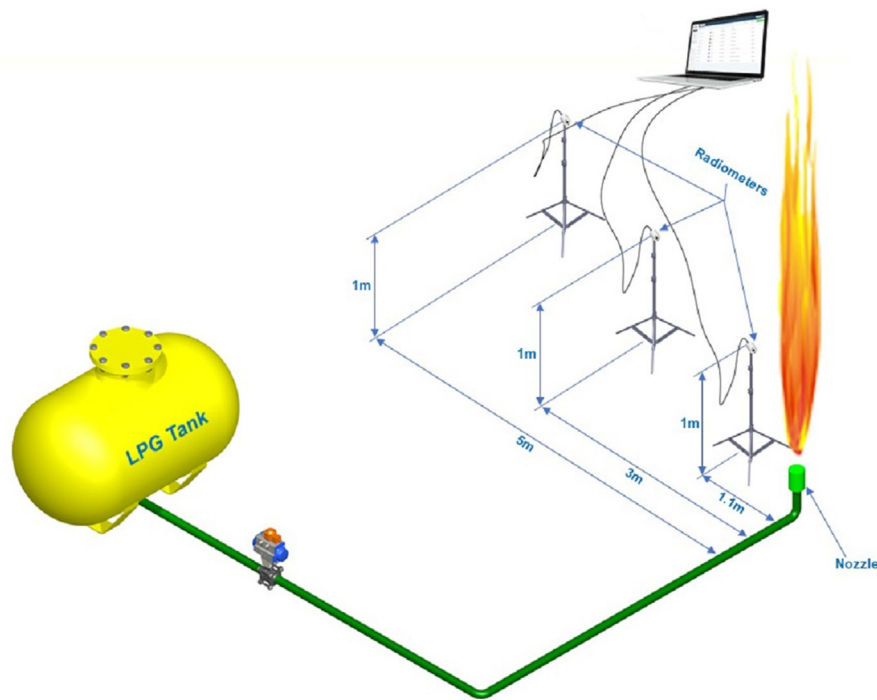
Figure 1. Scheme of the experimental setup.

shape at the center of the cylinder bottom to evaluate and characterize the better than radiation model, as illustrated in Figure 2. The simulation conditions were 303 K, 298 K, 1 atm, and 12.75 mm as air temperature, initial fuel temperature, absolute pressure, and inlet nozzle diameter, respectively. Under sonic velocities, large-scale vertical propane jet fires were developed in the open field. The propane fuel with an inlet velocity (mass flow rates) of 252.75 m s^{-1} (0.24 kg s^{-1}) to 254.51 m s^{-1} (0.08 kg s^{-1}) were tested. The steady-state simulation was conducted by considering gravity in the opposite path of the fuel flow injection and the time parameter for the different conditions was ignoring. The convergence criteria for the properties of boundary conditions were considered 10^{-4} to ensure observation of any remarkable change. A system including double 24-core 3.33 GHz processors with 48 GB RAM solved the governing equations. The incident radiation from the propane jet fires was compared for different models with a home code coupling with ANSYS CFX 15.0 software. The equations of energy, momentum, and mass balances and combustion equations were simultaneously solved. The mass flow rate fuel was presumed as the initial condition to initialize the solution of the equations. Figure 3 illustrates the solution algorithm of a propane jet fire simulation.

4.2. Mesh independency test

The computational domain is a symmetrical cylinder with a hexahedra mesh structure, which has a diameter and height of 10 m and 8 m, respectively. The meshes are expanded to 1.2 in both vertical and radial directions. The boundary condition of open pressure was employed in both cylinder top and shell. The experimental results were simulated with the MC and SST radiation and turbulence models, respectively, because of less computational time (Mashhadimoslem et al., 2020a,b; Santos and Lani, 2016; Tessé et al., 2004). The mesh independency test was performed using the grid convergence index (GCI) method from Roache et al. (1986), which is based on the use of the Richardson's generalization. In both the radial and vertical directions, the mesh extended 1.2 mm. The mesh was made up of 64 radial cells and 120 vertical cells. Based on this method, the mesh numbers of 500400, 907361, 1390000, and 2628000 were investigated. Based on this

approach, the stated number of elements in Table 3 was selected. The predicted findings were compared to the experimental values in Table 3. Because of its precision and lower computational time than the other tested values, the mesh number of 1,390,000 was selected as the best mesh dimension.

5. Result and discussion

5.1. Comparison of incident radiation adjacent to the jet flame axis

The effects of different radiation models on simulation, its comparison with the experimental results, and the predicted radiation are discussed. As stated in section 3, the obtained incident radiation was
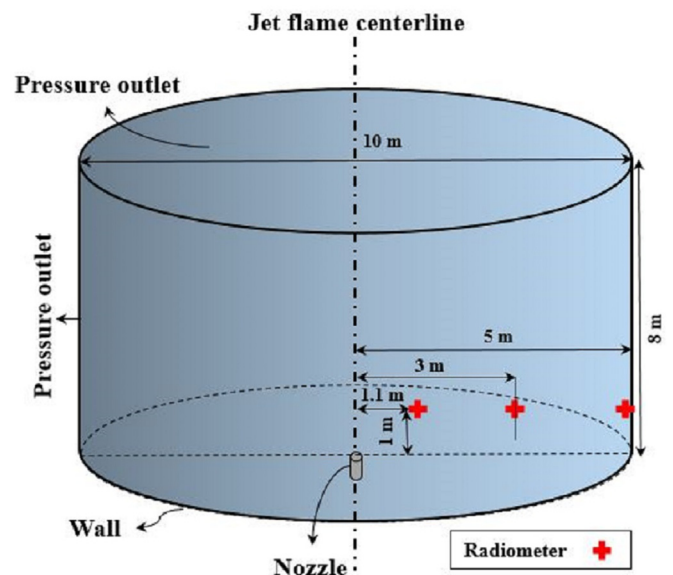

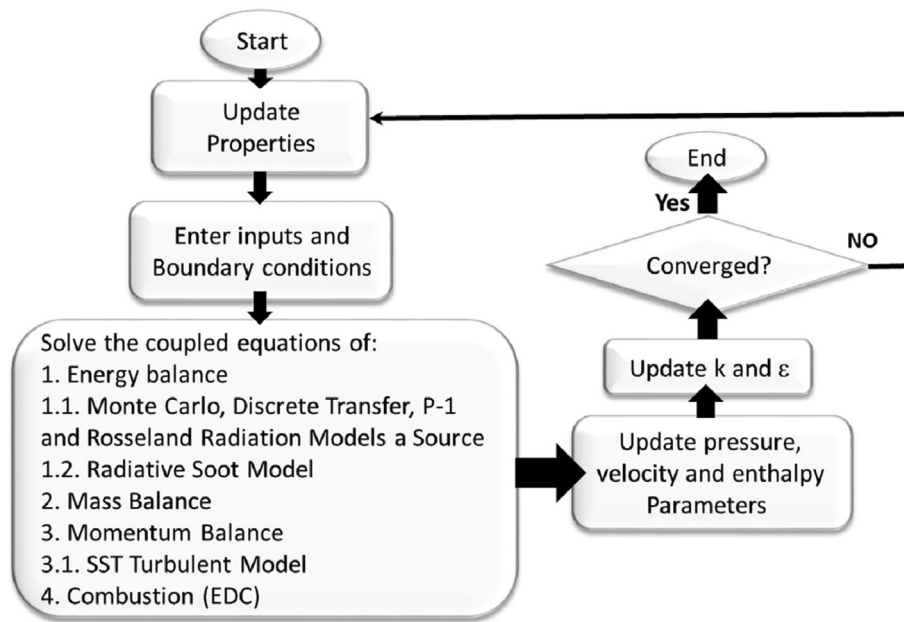**Figure 2.** Computational domain containing the boundary conditions.

Figure 3. Solution algorithm for the governing equations.

Table 3. Mesh independency test, based on GCI indicator.

Mesh No.	Element No.	GCI (Mesh Number 1; Mesh Number 2)	GCI	Predicted flame height (m)	Experimental flame height (m)
1	500,400	GCI (135,168; 404,928)	0.1952	4.31	5.7
2	907,361	GCI (404,928; 947,700)	0.0137	5.78	5.7
3	1,390,000	GCI (947,700; 2,035,400)	0.0100	5.71	5.7
4	2,628,000	-	-	-	-

recorded by radiometers placed at three different positions from the vertical propane jet flame. The locations were 1.1, 3, and 5 m from the release nozzle at the height of 1 m above the nozzle. The simulated data of the Monte Carlo (MC), DT, and P-1 radiation models are compared with the experimental ones, as displayed in Figure 4.

From Figure 4, according to the MC radiation solving method, which is a random function, the amount of thermal radiation simulated is in better agreement with the experimental data. The P-1 model has the lowest prediction accuracy at distances close to the jet flame axis (1.16 m), while at distances farther from the jet flame axis (5m), all radiation models show good predictions. Table 4 reports the average relative error range results of Figure 4 (a, b, c) for the radiation models simulation. For the propane jet fire, the average relative error range was 4.55 %–5.98 % for the MC radiation model in the fuel range velocities. The same results were obtained for DT and P-1 models with an error range of 6.33–12.6 % and 6.16–131.7 %, respectively. The MC model has a lower error than that for the DT and P-1 under the same conditions. According to the simulation data, the estimated radiation quantities at distances less than 3 m, the MC model have less error than the other models. At the position of 5 m, the anticipated radiation values for all models are close to the experimental data. Due to the high error of the P-1 radiation model adjacent to the jet flame body, the simulation data demonstrated that the DT and MC radiation models could estimate the quantity of radiation around the jet flame. The average absolute value of the relative error calculated was by Eq. (22):

$$AARE = \frac{1}{n} \sum_{i=1}^{n} \left| \frac{Xexp. - Xsim.}{Xexp.} \right| \qquad (22)$$

5.2. Comparison of incident radiation profile and contour

The incident radiation contours of propane jet flames, using the maximum and minimum inlet velocities at the same conditions, were simulated by different radiation models (i.e., P-1, MC, and DT radiation models). The simulations obtained are shown in Figures 5, 6, and 7. Due to the method of solving equations in different methods, the results are also different. Differential prediction, also known as P-1, is a reduction of the RTE model, which assumes that the intensity of isotropic radiation or direction is independent in a given spatial region. In another method, for each ray from solid boundaries to another boundary in geometry, the DT approach solves the radiative transfer equation of the RTE model. But in the MC approach, counting the number of photons occurring on a surface can determine the absorbed flux and average radiation flux.

As depicted in Figure 5, the contour of the P-1 radiation model is regular, though, according to the results of Figure 4, the radiation predicted by the P-1 radiation model has a higher error than the experimental data. The surface of the fire is changing due to the nature and phenomena of jet fire, which involves turbulence flow and combustion changes during the jet flame. The MC and DT radiation models seem to be fairly consistent with the observed evidence based on jet fire surface variations and jet flame fluctuation. Table 5 lists the error results of Figure 4 (a, b, c) for the minimum and maximum of inlet velocities. The average absolute value of the relative error was computed by Eq. (22).

The MC radiation model simulation results had an error of about 10 % with experimental data. Based on the observations, the contour levels of incident radiation for DT and MC are much greater than for P-1. The DT and P-1 radiation models simulation results had an error of about 13%
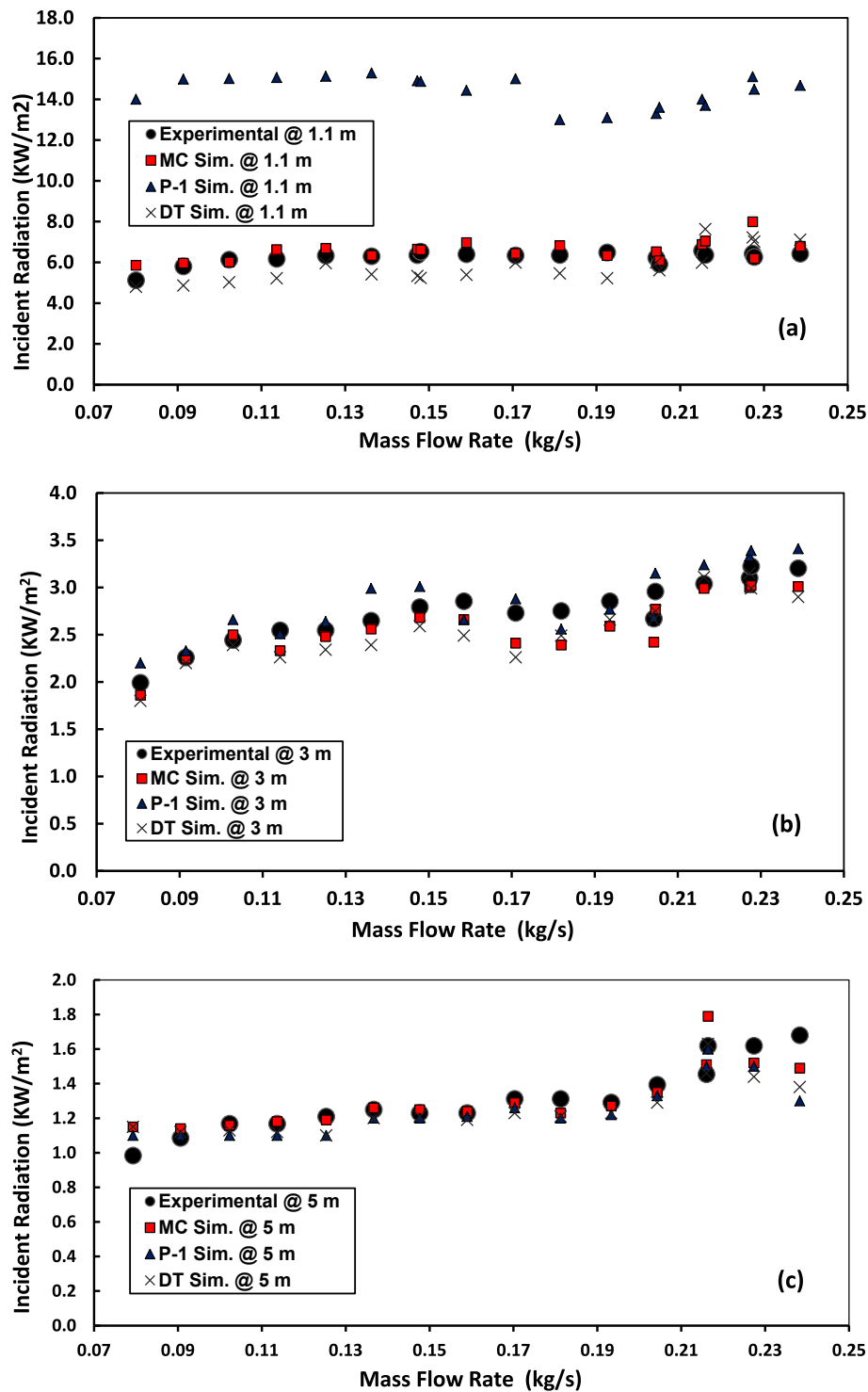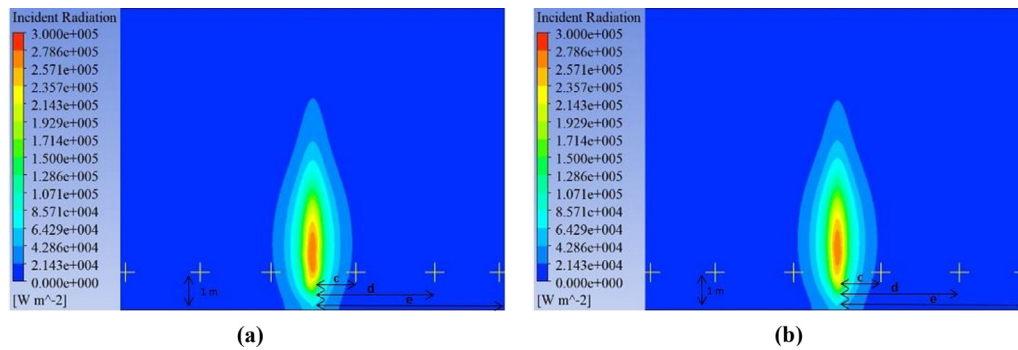
Figure 4. Comparison of incident radiation models at (a) 1.1 m, (b) 3 m, and (c) 5 m as the radiometer positions in terms of distance from the jet flame axis.

Table 4. Comparison between the predicted and experimental results shown in Figure 4.

| Radiation model simulation	AARE (%) For 1.1 m	AARE (%) For 3 m	AARE (%) For 5 m
MC	5.97	5.98	4.55
DT	12.6	7.36	6.33
P-1	131.7	6.08	6.16

Figure 5. Incident radiation jet flame contours predicted by the P-1 radiation model, under different velocities: (a) 252.75 m/s, and (b) 254.51 m/s. The radiometers were horizontally located at (c) 1.1 m, (d) 3 m and (e) 5 m.
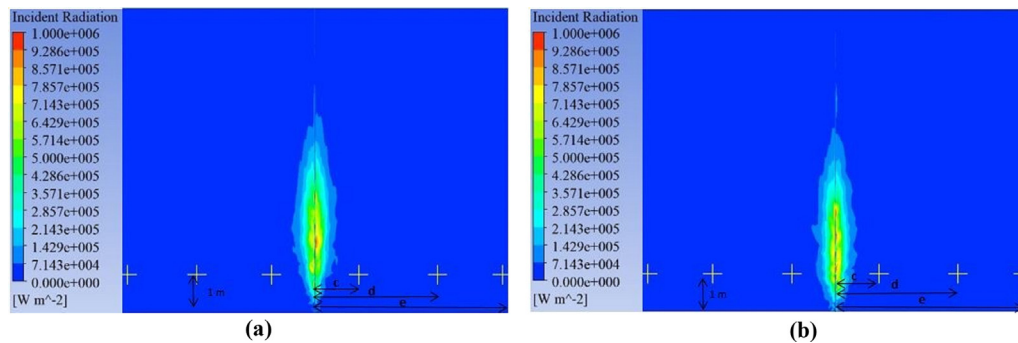
Figure 6. Incident radiation jet flame contours predicted by the MC radiation model, under different velocities: (a) 252.75 m/s, and (b) 254.51 m/s. The radiometers were horizontally located at (c) 1.1 m, (d) 3 m and (e) 5 m.
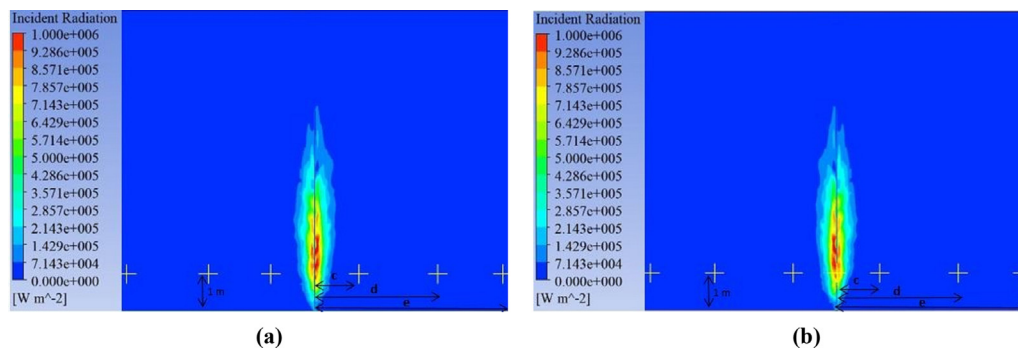
Figure 7. Incident radiation jet flame contours predicted by the DT radiation model, under different velocities: (a) 252.75 m/s, and (b) 254.51 m/s. The radiometers were horizontally located at (c) 1.1 m, (d) 3 m and (e) 5 m.
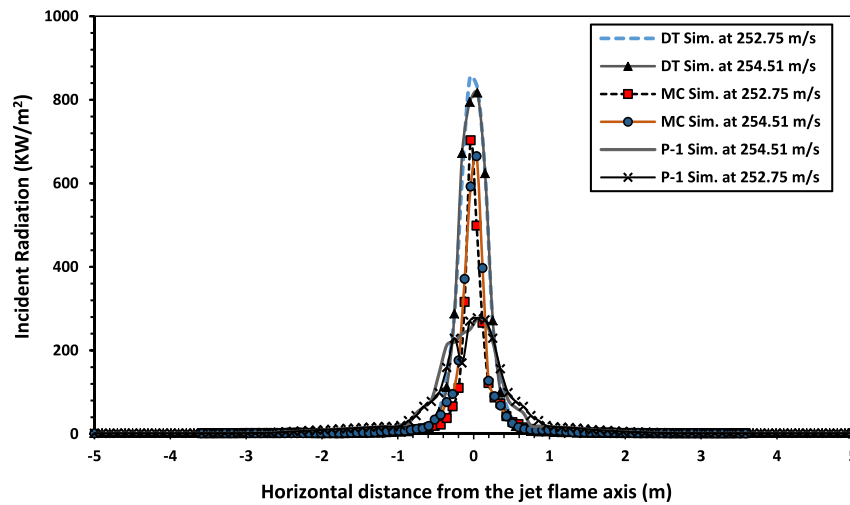
and 56% with experimental data, respectively. The simulation predictions illustrated that the DT and MC radiation models are more suitable for predicting the quantity of radiation around the jet flame owing to the high error of the P-1 model adjacent to the jet flame. Figure 8 and sections 5.2 reveal the maximum incident radiation of 852 kW/m^2, 669 kW/m^2, and 278 kW/m^2 for DT, MC, and P-1 models in terms of the distance relative to the jet flame location, respectively.

The estimated radiation by two MC and DT models inside the jet flame is above 600 kW/m^2. Given the limitations in instruments determining the amount of radiation, the simulation results in Figure 8

Table 5. Comparison of the estimated and experimental data shown in Figure 7.

Radiation model simulation	Jet Fire Velocity (m/s)	Jet Fire Mass flow rate (kg/s)	Max Incident Radiation predicted of jet flame (kW/m^2)	Average predicted Incident Radiation at radiometers (kW/m^2)	Average Experimental jet flame Incident Radiation at radiometers (kW/m^2)	AARE (%) For Incident Radiation
MC	252.75	0.24	1117.6	2.9	2.7	12.7
DT	252.75	0.24	936.1	2.6	2.7	15
P-1	252.75	0.24	277.4	5.8	2.7	65
MC	254.51	0.08	1057.5	3.6	3.75	9.33
DT	254.51	0.08	949.4	4	3.75	11
P-1	254.51	0.08	272.5	6.13	3.75	47.7

Figure 8. Comparison of the estimated incident radiation profile by the simulation under the same conditions by MC, DT and P-1 models from surfaces placed at 1 m above the release orifice.

indicate that the quantity of radiation along the jet flame axis can be anticipated. A lack of accurate prediction for the jet flame temperatures was found through the simulations by the Rosseland model. This model is a simplified form of the RTE equation for the case of an optically thick media. The Rosseland estimation is introduced by the energy transport equation and the heat flux radiation conduction (Rosseland, 1936). The Rosseland method calculate the energy spectrum for the radiation emitted by a blackbody. By considering the Rosseland radiation model approximation is not valid in the vicinity of walls (ANSYS CFX-Solver Theory Guide; 2017), it cannot be explained. The maximum temperature for the jet flame centerline estimated by the Rosseland model was 1350 K; while the maximum temperature for the jet flame axis estimated by the MC, DT, P-1 models range was between 1834 and 1945 K, which is within the range of the experimental data acquired by Palacios et al. (2009) (the range of 1700–1900 K). Therefore, the Rosseland radiation model is not suitable for simulating the open field of large-scale vertical propane jet fire.

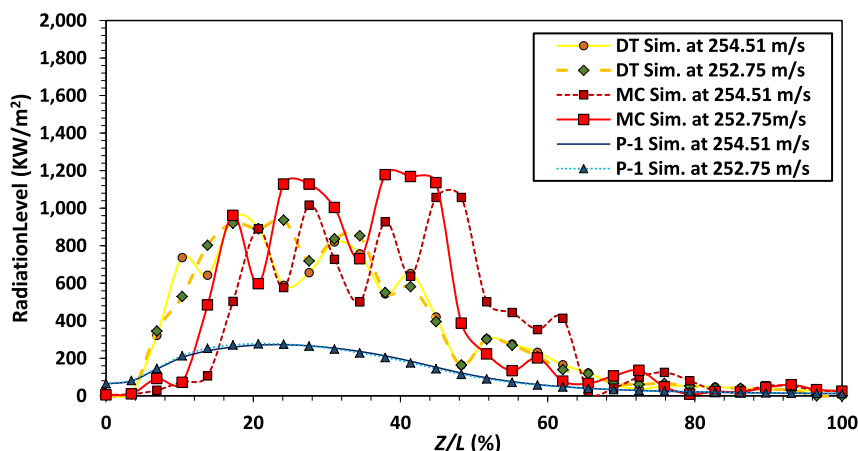### 5.3. Comparison of axial incident radiation profile

The change in the emitted radiation quantities, along the axial jet flame length, is plotted versus the dimensionless centerline jet flame length, *Z/L*, in Figure 9.

Figure 9 indicates that the radiation rate is enhanced at the initial positions of the jet flame and then reduces at the top of the jet flame. The

simulated results for the incident radiation along the jet flame axis, using the maximum and minimum fuel exit velocities, have shown to be well predicted by the DT model. The MC model is a random function where the quantity of the estimated radiation changes randomly as the input speed varies. So, due to the jet flame fluctuation, satisfying agreements between empirical and MC radiation model-simulated data have been detected (Mashhadimoslem et al., 2020b). Since the DT model's simulations display convergence at various inlet velocities, it appears that this model can also be used to estimate the amount of radiation along the jet flame length. The simulation-based data in Figure 9 show that both radiation models of DT and MC have got the same prediction after 70 % of the jet flame length. The results also exhibited that the radiation estimated by the P-1 model has more initial values than the other ones, but during the jet flame, the maximum estimated radiation is about 270 kW/m^2. Therefore, it is best to consider the Monte Carlo and DT models for propane jet fire simulation, based on the results in Sections 5.1, 5.2, and Figure 9.

6. Conclusions

In the current study, a vertical propane jet fire was simulated by four radiation models: The P-1, Monte Carlo (MC), Discrete Transfer (DT), and Rosseland radiation. The predicted incident radiation jet fire of propane in the open field is verified by the empirical data, extracted by radiometers at three points placed at different distances.

Figure 9. Simulations for the axial incident radiation profile of jet flames, using three different radiation models.

1. Among three radiation models of the P-1, DT, and MC, the MC model was the best one in the prediction of experimental incident radiation with an acceptable relative error of 5 %.
2. Due to the error of less than 15 % predicted by MC and DT models, these radiation models can simulate the jet flame length with good precision.
3. The simulation results revealed that at close distances (about one meter) of the vertical jet fire, due to the relatively high error above 65%, Because of the lack of radiation prediction accuracy of jet fire, the P-1 radiation model for the open field of large-scale vertical propane jet is not suitable for simulation.
4. The Rosseland radiation model is not suitable for simulating the open field of large-scale vertical propane jet fire.

The simulation and accurate estimation of jet fire radiation are very significant in process industries because of determining the proper and secure area for the equipment, tanks, and buildings. Another benefit is that this offers higher reliability on the CFD simulation as prediction, leading to more accurate predictions of jet fire radiation in the process industries.

According to the findings of this study, for a more accurate simulation of propane jet fire in the open field, the MC radiation model is used. Since radiation measurement in the jet flame center is limited, CFD simulation can be useful in estimating radiation in the jet flame center. The potential application of the present study is the accurate prediction of propane jet flame radiation in oil and gas industries congested areas in order to consequence risk analysis.

Declarations

Author contribution statement

Funding statement

Data availability statement

Data included in article/supp. material/referenced in article

Declaration of interests statement

The authors declare no conflict of interest.

Additional information

No additional information is available for this paper.

References

ANSYS, C.F.X., 2009. ANSYS CFX-solver theory guide, 15317. ANSYS CFX Release, pp. 724–746.

Baalisampang, T., Abbassi, R., Garaniya, V., Khan, F., Dadashzadeh, M., 2017. Fire impact assessment in FLNG processing facilities using Computational Fluid Dynamics (CFD). Fire Saf. J. 92, 42–52.

Bird, R.B., Stewart, W.E., Lightfoot, E.N., 2007. Transport Phenomena, Revised, 12. J. Wiley & Sons, p. 905.

Brzustowski, T.A., 1973. Predicting Radiant Heating from Flares.

Chamberlain, G.A., 1987. Developments in design methods for predicting thermal radiation from flares. Chem. Eng. Res. Des. 65 (4).

Cirrone, D.M.C., Makarov, D., Molkov, V., 2019a. Thermal radiation from cryogenic hydrogen jet fires. Int. J. Hydrogen Energy 44 (17), 8874–8885.

Cirrone, D.M.C., Makarov, D., Molkov, V., 2019b. Simulation of thermal hazards from hydrogen under-expanded jet fire. Int. J. Hydrogen Energy 44 (17), 8886–8892.

Consalvi, J.L., Nmira, F., 2017. Absorption turbulence-radiation interactions in sooting turbulent jet flames. J. Quant. Spectrosc. Radiat. Transf. 201, 1–9.

Cook, J., Bahrami, Z., Whitehouse, R.J., 1990. A comprehensive program for calculation of flame radiation levels. J. Loss Prev. Process. Ind. 3 (1), 150–155.

Cumber, P.S., Fairweather, M., 2005. Evaluation of flame emission models combined with the discrete transfer method for combustion system simulation. Int. J. Heat Mass Tran. 48 (25-26), 5221–5239.

Cumber, P.S., Onokpe, O., 2013. Turbulent radiation interaction in jet flames: sensitivity to the PDF. Int. J. Heat Mass Tran. 57 (1), 250–264.

Cumber, P.S., Spearpoint, M., 2006. A computational flame length methodology for propane jet fires. Fire Saf. J. 41 (3), 215–228.

Galant, S., Grouset, D., Martinez, G., 1984. Comparison between test results and the API Guidelines. In: Third International Flare System Seminar.

Gómez-Mares, M., Munoz, M., Casal, J., 2009. Axial temperature distribution in vertical jet fires. J. Hazard Mater. 172 (1), 54–60.

Gómez-Mares, M., Muñoz, M., Casal, J., 2010. Radiant heat from propane jet fires. Exp. Therm. Fluid Sci. 34 (3), 323–329.

Gosman, A.D., Lockwood, F.C., Megahed, I.E.A., Shah, N.G., 1982. Prediction of the flow, reaction, and heat transfer in a glass furnace. J. Energy 6 (6), 353–360.

Habibi, A., Merci, B., Heynderickx, G.J., 2007 Nov 1. Impact of radiation models in CFD simulations of steam cracking furnaces. Comput. Chem. Eng. 31 (11), 1389–1406.

Hottel, H.C., Hawthorne, W.R., 1948. January. Diffusion in laminar flame jets. In: Symposium on Combustion and Flame, and Explosion Phenomena, 3. Elsevier, pp. 254–266. No.1.

Hussein, H.G., Brennan, S., Shentsov, V., Makarov, D., Molkov, V., 2018. Numerical validation of pressure peaking from an ignited hydrogen release in a laboratory-scale enclosure and application to a garage scenario. Int. J. Hydrogen Energy 43 (37), 17954–17968.

Hustad, J.E., Sonju, O.K., 1986. Radiation and size scaling of large gas and gas/oil diffusion flames. In: Am. Inst Aeronaut. Astronaut., Tenth Int. Coll. Dynamics of Explosions and Reactive Systems, Berkeley, p. 365.

Jang, C.B., Choi, S.W., 2017. Simulation and damage analysis of an accidental jet fire in a high-pressure compressed pump shelter. Safety Health Work 8 (1), 42–48.

Jang, C.B., Jung, S., 2016. Numerical computation of a large-scale jet fire of high-pressure hydrogen in process plant. Energy Sci. Eng. 4 (6), 406–417.

Jang, C.B., Choi, S.W., Baek, J.B., 2015. CFD modeling and fire damage analysis of jet fire on hydrogen pipeline in a pipe rack structure. Int. J. Hydrogen Energy 40 (45), 15760–15772.

Jeans, J.H., 1917. Stars, gaseous, radiative transfer of energy, 78. Monthly Notices of the Royal Astronomical Society, pp. 28–36.

Jeon, M.K., Cho, M.S., Lee, M.J., Kim, N.I., Ryou, H.S., 2015. Effects of propane pyrolysis on basic flame structures of non-premixed jet flame. J. Mech. Sci. Technol. 29 (9), 4053–4059.

Kleiveland, R.N., 2005. Modelling of Soot Formation and Oxidation in Turbulent Diffusion Flames.

Li, G., Modest, M.F., 2003. Importance of turbulence-radiation interactions in turbulent diffusion jet flames. J. Heat Tran. 125 (5), 831–838.

Liu, Y., Moser, A., Sinai, Y., 2004. Comparison of a CFD fire model against a ventilated fire experiment in an enclosure. Int. J. Vent. 3 (2), 169–181.

Liu, J., Wang, J., Chen, M., 2019. Estimating the trajectory length of buoyant turbulent jet flames issuing from a downward sloping nozzle. Process Saf. Environ. Protect. 132, 153–159.

Lowesmith, B.J., Hankinson, G., 2012. Large scale high pressure jet fires involving natural gas and natural gas/hydrogen mixtures. Process Saf. Environ. Protect. 90 (2), 108–120.

Lowesmith, B.J., Hankinson, G., Acton, M.R., Chamberlain, G., 2007. An overview of the nature of hydrocarbon jet fire hazards in the oil and gas industry and a simplified approach to assessing the hazards. Process Saf. Environ. Protect. 85 (3), 207–220.

Magnussen, B., 1981. January. On the structure of turbulence and a generalized eddy dissipation concept for chemical reaction in turbulent flow. In: 19th Aerospace Sciences Meeting, p. 42.

Magnussen, B.F., 1989. June. Modeling of pollutant formation in gas turbine combustors based on the eddy dissipation concept. In: Eighteenth International Congress on Combustion Engines, Tianjin, China.

Mashhadimoslem, H., Ghaemi, A., Behroozi, A.H., Palacios, A., 2020a. A New simplified calculation model of geometric thermal features of a vertical propane jet fire based on experimental and computational studies. Process Saf. Environ. Protect. 135, 301–314.

Mashhadimoslem, H., Ghaemi, A., Palacios, A., Behroozi, A.H., 2020b. A new method for comparison thermal radiation on large-scale hydrogen and propane jet fires based on experimental and computational studies. Fuel 282, 118864.

Mbainguebem, A., Mouangue, R., Bianzeube, B.T., 2017. CFD studies of soot production in a coflow laminar diffusion flame under conditions of micro-gravity in fire safety. J. Taibah Univ. Sci. 11 (4), 566–575.

McCaffrey, B.J., Evans, D.D., 1988. January. Very large methane jet diffusion flames. In: Symposium (International) on Combustion, 21. Elsevier, pp. 25–31. No. 1.

McMurray, R., 1982. Flare radiation estimated. Hydrocarb. Process. (United States) 61 (11).

Mehta, R.S., Connell Haworth, Daniel, Modest, M.F., 2010. Composition PDF/photon Monte Carlo modeling of moderately sooting turbulent jet flames. Combust. Flame 157 (5), 982–994.

Palacios, A., Casal, J., 2011. Assessment of the shape of vertical jet fires. Fuel 90 (2), 824–833.

Palacios, A., Rengel, B., 2020. Computational analysis of vertical and horizontal jet fires. J. Loss Prev. Process. Ind. 65, 104096.

Palacios, A., Muñoz, M., Casal, J., 2009. Jet fires: an experimental study of the main geometrical features of the flame in subsonic and sonic regimes. AIChE J. 55 (1), 256–263.

Palacios, A., Muñoz, M., Darbra, R.M., Casal, J., 2012. Thermal radiation from vertical jet fires. Fire Saf. J. 51, 93–101.

Palacios Rosas, A., 2011. Study of Jet Fires Geometry and Radiative Features. Universitat Politècnica de Catalunya.

Petera, K., Dostál, M., 2016. Heat transfer measurements and CFD simulations of an impinging jet. In: EPJ Web of Conferences, 114. EDP Sciences, 02091.

Pope, S.B., 2001. Turbulent Flows.

Roache, P.J., Ghia, K.N., White, F.M., 1986. Editorial Policy Statement on the Control of Numerical Accuracy.

Rosseland, S., 1936. Theoretical Astrophysics; Atomic Theory and the Analysis of Stellar Atmospheres and Envelopes. Clarendon.

Rusch, D., Blum, L., Moser, A., Rösgen, T., 2008. Turbulence model validation for fire simulation by CFD and experimental investigation of a hot jet in crossflow. Fire Saf. J. 43 (6), 429–441.

Santos, P.D., Lani, A., 2016. An object-oriented implementation of a parallel Monte Carlo code for radiation transport. Comput. Phys. Commun. 202, 233–261.

Schuller, R.B., Hustad, J., Nylund, J., Sonju, O.K., 1983. Effect of Nozzle Geometry on Burning Subsonic Hydrocarbon Jets (No. CONF-830702-). Research Division Det norske Veritas Hoevik, Norway.

Taghinia, J., Rahman, M.M., Siikonen, T., 2016. CFD study of turbulent jet impingement on curved surface. Chin. J. Chem. Eng. 24 (5), 588–596.

Tessé, L., Dupoirieux, F., Taine, J., 2004. Monte Carlo modeling of radiative transfer in a turbulent sooty flame. Int. J. Heat Mass Tran. 47 (3), 555–572.

Wang, C.J., 2012. Simulation of heptane jet fire at low atmosphere pressure. In: Advanced Materials Research, 516. Trans Tech Publications Ltd, pp. 1070–1073.

Wang, C., Guo, J., 2011. Computer simulation of liquid jet fire with various injection conditions. Procedia Engineering 15, 3942–3947.

Wang, C.J., Wen, J.X., Chen, Z.B., Dembele, S., 2014. Predicting radiative characteristics of hydrogen and hydrogen/methane jet fires using FireFOAM. Int. J. Hydrogen Energy 39 (35), 20560–20569.

Wang, Z., Zhou, K., Zhang, L., Nie, X., Wu, Y., Jiang, J., Dederichs, A.S., He, L., 2021. Flame extension area and temperature profile of horizontal jet fire impinging on a vertical plate. Process Saf. Environ. Protect. 147, 547–558.

Xiao, J., Kuznetsov, M., Travis, J.R., 2018. Experimental and numerical investigations of hydrogen jet fire in a vented compartment. Int. J. Hydrogen Energy 43 (21), 10167–10184.

Yeoh, G.H., Yuen, K.K., 2009. Computational Fluid Dynamics in Fire Engineering: Theory, Modelling and Practice. Butterworth-Heinemann.

Yuen, A.C.Y., Yeoh, G.H., Yuen, R.K.K., Chen, T., 2013. Numerical simulation of a ceiling jet fire in a large compartment. Procedia Engineering 52, 3–12.

Zárate, L.G., Lara, H.E., Cordero, M.E., Kozanoglu, B., 2014. Infrared thermography and CFD analysis of hydrocarbon jet fires. Chem Eng Trans 39.

Zhou, K., Jiang, J., 2016. Thermal radiation from vertical turbulent jet flame: line source model. J. Heat Tran. 138 (4).